Molecular Therapy
Nucleic Acids
Original Article

circRNA hsa_circ_0018414 inhibits the progression of LUAD by sponging miR-6807-3p and upregulating DKK1

Yuanshan Yao,[1] Yinjie Zhou,[1] and Qingwang Hua[1]

[1]Department of Thoracic Surgery, Hwa Mei Hospital, University of Chinese Academy of Sciences (Ningbo No. 2 Hospital), Haishu District, Ningbo, Zhejiang 315010, China

Lung adenocarcinoma (LUAD) is a subtype of lung cancer with a high incidence and mortality all over the world. In recent years, circular RNAs (circRNAs) have been verified to be a novel subtype of noncoding RNAs that exert vital functions in various cancers. Our research was designed to investigate the role of circ_0018414 in LUAD. We first observed that circ_0018414 was downregulated in LUAD tissues and cells. Also, low expression of circ_0018414 predicted unfavorable prognosis of LUAD patients. Then, upregulation of circ_0018414 repressed cell proliferation and stemness, while promoting cell apoptosis, in LUAD. Moreover, circ_0018414 overexpression enhanced the expression of its host gene, dickkopf WNT signaling pathway inhibitor 1 (DKK1), therefore inactivating the Wnt/β-catenin pathway. Additionally, circ_0018414 could sponge miR-6807-3p to protect DKK1 mRNA from miR-6807-3p-induced silencing, leading to DKK1 upregulation in LUAD cells. Finally, rescue assays proved that circ_0018414 inhibited the progression of LUAD via the miR-6807-3p/DKK1 axis-inactivated Wnt/β-catenin pathway. The findings in our work indicated circ_0018414 as a tumor inhibitor in LUAD, which might provide a new perspective for LUAD treatment.

INTRODUCTION

As one of the most prevalent and deadly cancers globally,[1] lung cancer can be mainly divided into two types: non-small cell lung cancer accounts for about 85%, and small cell lung cancer accounts for about 15%. Lung adenocarcinoma (LUAD) is a subtype of non-small cell lung cancer, which is the deadliest disease among never-smokers around the world.[2,3] Despite extensive research on LUAD treatment (including surgical resection, chemotherapy, and targeted therapy), the 5-year survival rate of patients with LUAD remains terrible.[4] Thus, there is an urgent need to identify novel biology markers for LUAD treatment.

Circular RNAs (circRNAs) are a newly discovered subtype of noncoding RNAs, which were first discovered in 1976 in an RNA virus.[5,6] circRNAs originate from the back-splicing of messenger RNAs (mRNAs) from their host genes. Compared with linear RNAs, circRNAs are featured by a closed loop with strengthened stability.[7] Actually, accumulating studies have demonstrated the pivotal roles of circRNAs in cancers. For instance, circRNA_102171 aggravates the progression of papillary thyroid cancer via activating the Wnt/β-catenin pathway in a CTNNBIP1-dependent way.[8] circRNA circ_100338 activates the mTOR signaling pathway in hepatocellular carcinoma (HCC) via targeting the miR-141-3p/RHEB axis.[9] circRNA circ_0008717 serves as an oncogene to contribute to osteosarcoma development via binding with miR-203.[10] circRNA circ_100269 is downregulated in gastric cancer cells and inhibits cell proliferation via serving as a sponge of miR-630.[11] circ_0018414 derived from dickkopf WNT signaling pathway inhibitor 1 (DKK1) is a novel circRNA that has never been explored in any cancer. The present study was designed to probe into the biological functions of circ_0018414 in LUAD.

Recently, some researchers have proposed that circRNAs could modulate cancer progression via sponging specific microRNAs (miRNAs) to reduce the inhibition of miRNAs on target mRNAs.[12] In this way, circRNAs serve as a competing endogenous RNA (ceRNA) to sponge miRNAs to boost the expression of target genes.[13] For instance, circRNA hsa_circ_104718 drives the progression of HCC via regulating the miR-218-5p/TXNDC5 signaling pathway.[14] circRNA circ_0025202 increases tamoxifen sensitivity and tumor formation in breast cancer via modulating the miR-182-5p/FOXO3a pathway.[15] circRNA hsa_circ_0006168 binds with miR-100 to modulate mTOR expression and therefore aggravate the progression of esophageal squamous cell carcinoma.[16] Also, circRNA UBAP2 promotes ovarian cancer progression by sponging miR-144 to upregulate CHD2 expression.[17] In our previous study, we focused on the interaction between circRNAs and the Wnt pathway in LUAD.[18,19] Based on our previous studies, we further detected the role of a circRNA derived from DKK1 (circ_0018414) and its association with the Wnt pathway in LUAD.

Received 29 April 2020; accepted 31 December 2020;
https://doi.org/10.1016/j.omtn.2020.12.031.

Correspondence: Qingwang Hua, Department of Thoracic Surgery, Hwa Mei Hospital, University of Chinese Academy of Sciences (Ningbo No. 2 Hospital), No. 41 Northwest Street, Haishu District, Ningbo, Zhejiang 315010, China.
E-mail: wangjihu3639696@163.com

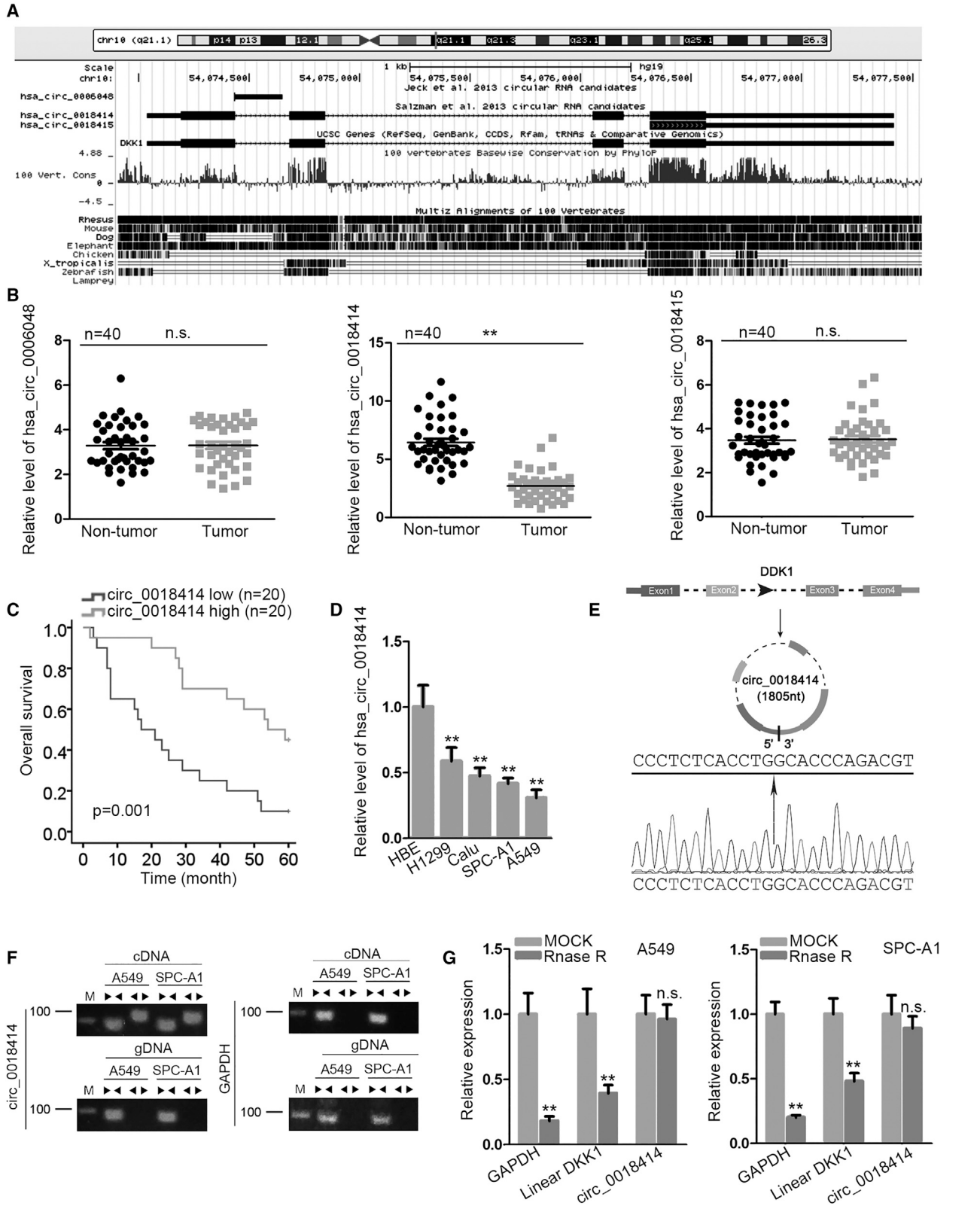

(legend on next page)

RESULTS

circ_0018414 was downregulated in LUAD, and low expression of circ_0018414 predicted poor prognosis of LUAD patients

DKK1 is a famous tumor suppressor in various cancers, such as breast cancer,[20] pituitary prolactinoma,[21] LUAD,[22] and so on. Our study aimed to study the role of circRNAs originating from DKK1 in LUAD. According to the UCSC (http://genome.ucsc.edu/) and circBase (http://www.circbase.org/) databases, there were three kinds of circRNAs derived from DKK1 (including circ_0006048, circ_0018414, and circ_0018415) (Figure 1A). By applying quantitative real-time polymerase chain reaction (PCR), expression of the above three circRNAs in LUAD tissues and adjacent non-tumor tissues was examined. It was demonstrated that the circ_0018414 level was decreased in LUAD tissues in comparison with adjacent non-tumor tissues, while circ_0006048 and circ_0018415 showed no significant differences between the two groups (Figure 1B). Then, we divided LUAD patients enrolled in this study into two groups (a circ_0018414 high-expressed group and a circ_0018414 low-expressed group) based on the median value of circ_0018414 expression. Kaplan-Meier analysis implied that low circ_0018414 was associated with unfavorable prognosis in LUAD patients (Figure 1C). Next, the expression of circ_0018414 was tested in LUAD cells (A549, SPC-A1, H1299, and Calu) relative to normal cells (HBE). Results showed that the circ_0018414 level was apparently reduced in LUAD cells (Figure 1D). Moreover, we sought to verify the circular characteristic of circ_0018414. The structure of circ_0018414 is presented in Figure 1E. Gel electrophoresis exposed that circ_0018414 was amplified by divergent primers only from cDNA instead of genomic DNA (gDNA) (Figure 1F). Furthermore, under the treatment of RNase R, the level of linear DKK1 was decreased while that of circ_0018414 showed no obvious change (Figure 1G). The results suggested that circ_0018414 was more difficult to be digested by RNase R than the linear DKK1, proving it was more stable than the linear form. In conclusion, circ_0018414 was downregulated in LUAD and low expression of it predicted poor prognosis of LUAD patients.

circ_0018414 served as an anti-oncogene in LUAD cells

To investigate the role of circ_0018414 in LUAD, a series of gain-of-function assays were conducted in LUAD cells. A549 and SPC-A1 cells were used for the following experiments since they expressed the lowest circ_0018414 level among the detected four LUAD cell lines. Thereafter, the above two LUAD cells were transfected with circ_0018414 overexpression vector, and quantitative real-time PCR validated the overexpression efficiency (Figure 2A). Next, a Cell Counting Kit-8 (CCK-8) assay was implemented and the results displayed that the proliferation ability of LUAD cells was attenuated by circ_0018414 upregulation (Figure 2B). Likewise, colony formation assay data showed that the number of colonies was notably reduced after overexpressing circ_0018414 in LUAD cells (Figure 2C). The outcomes of a 5-ethynyl-2′-deoxyuridine (EdU) assay also illustrated that LUAD cell proliferation was notably impaired due to circ_0018414 upregulation (Figure 2D). Moreover, the results of flow cytometry analysis exposed that the apoptosis rate of LUAD cells was markedly increased as a result of circ_0018414 overexpression (Figure 2E). Similarly, the results from a TUNEL (terminal deoxynucleotidyl transferase-mediated deoxyuridine triphosphate nick end labeling) assay indicated that LUAD cell apoptosis was enhanced under the overexpression of circ_0018414 (Figure 2F). Furthermore, JC-1 staining assay data revealed that upregulation of circ_0018414 decreased mitochondrial membrane potential in LUAD cells (Figure 2G). Taken together, circ_0018414 upregulation hindered cell proliferation and promoted cell apoptosis in LUAD.

In the meantime, we also knocked down circ_0018414 in H1299 cells to further test its role in LUAD. The quantitative real-time PCR data verified the knockdown efficiency of circ_0018414 (Figure S1A). The outcomes of cell proliferation assays, including CCK-8, colony formation, and EdU assays, showed that LUAD cell proliferative ability was increased due to circ_0018414 depletion (Figures S1B–S1D). Data from flow cytometry analysis and a TUNEL assay demonstrated that LUAD cell apoptosis was depressed resulting from circ_0018414 deficiency (Figures S1E and S1F). In summary, circ_0018414 downregulation facilitated cell proliferation and repressed cell apoptosis in LUAD cells.

circ_0018414 regulated DKK1 expression and inactivated the Wnt/β-catenin signaling pathway

Thereafter, we aimed to investigate whether circ_0018414 had effects on the expression of its host gene DKK1. Both the data from nuclear-cytoplasmic fractionation and fluorescence *in situ* hybridization (FISH) assays validated that circ_0018414 was predominantly distributed in the cytoplasm of LUAD cells (Figures 3A and 3B), implying that circ_0018414 might elicit post-transcriptional regulation on genes in LUAD cells. Next, the mRNA level of DKK1 was found to be increased by circ_0018414 upregulation (Figure 3C). However, DKK1 overexpression had no remarkable influence on the expression of circ_0018414 in LUAD cells (Figure 3D). As anticipated, we discovered that luciferase activity of the DKK1 promoter had no obvious response to circ_0018414 upregulation (Figure 3E), implying

Figure 1. circ_0018414 was downregulated in LUAD, and low expression of circ_0018414 predicted poor prognosis of LUAD patients

(A) Diagram from the UCSC database presented three circRNAs (hsa_circ_0006048, hsa_circ_0018414, and hsa_circ_0018415) derived from DKK1. (B) Quantitative real-time PCR detected the expression of hsa_circ_0006048, hsa_circ_0018414, and hsa_circ_0018415 in 40 pairs of LUAD tissues. Paired Student's t test. (C) The association of circ_0018414 expression with the overall survival of LUAD patients was analyzed by the Kaplan-Meier method. Log-rank test. (D) Quantitative real-time PCR revealed the expression of circ_0018414 in LUAD cells (A549, SPC-A1, H1299, and Calu) relative to normal cells (HBE). One-way ANOVA. (E) Schematic diagram showed the structure of circ_0018414, and Sanger sequencing detected the splicing junction of circ_0018414. (F) Gel electrophoresis tested the products by divergent or convergent primers amplified from cDNA or gDNA. (G) Quantitative real-time PCR detected the expression of circ_0018414 and linear DKK1 mRNA in LUAD cells under the treatment with RNase R, with the mock group as a negative control (NC). Unpaired Student's t test. $^{**}p < 0.01$. n.s., not significant. Error bars indicate SD; n = 5 in each experiment.

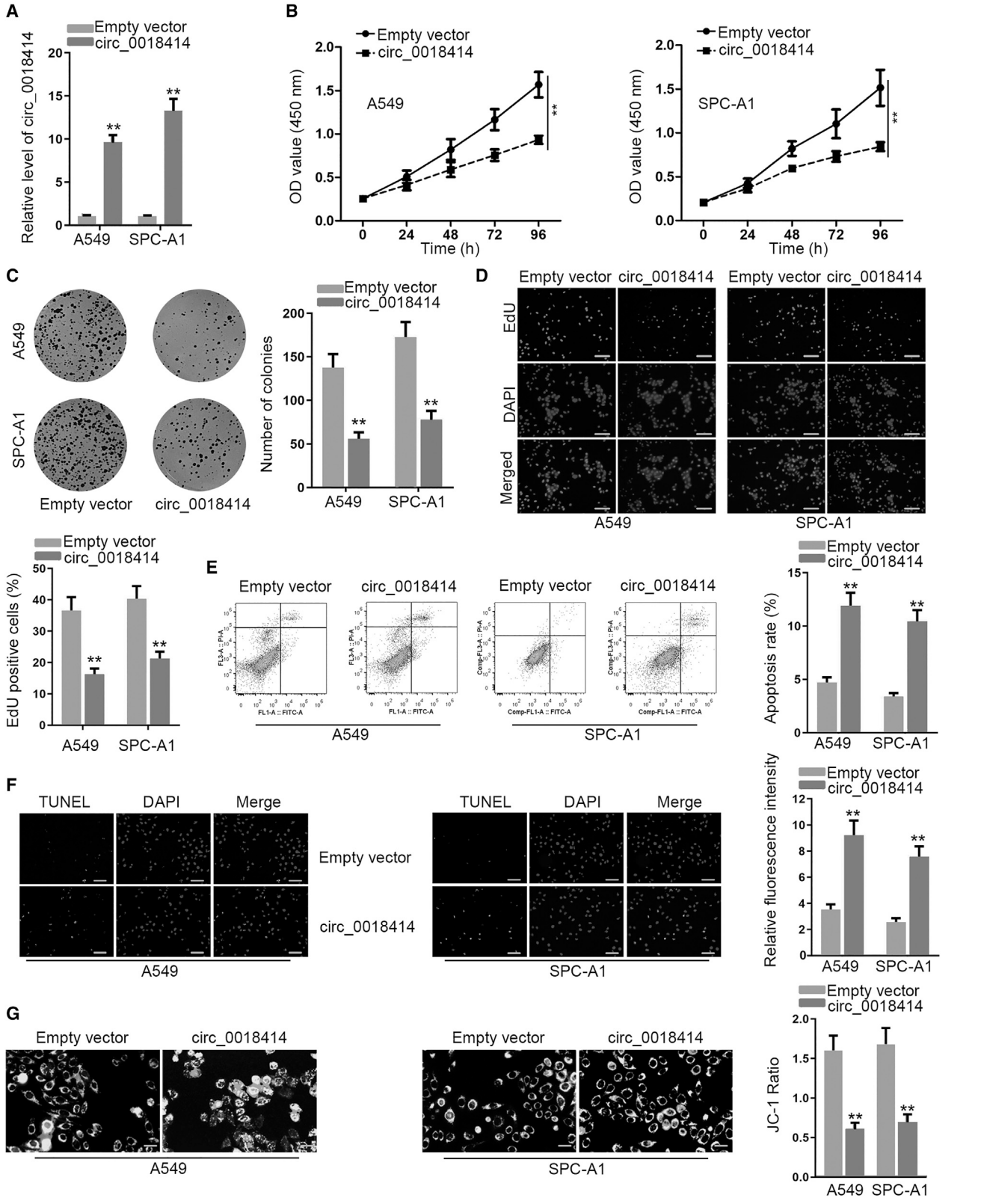

(legend on next page)

that circ_0018414 modulated DKK1 at the post-transcriptional level rather than at the transcriptional level. Additionally, RNA immunoprecipitation (RIP) assay data showed that both circ_0018414 and DKK1 were remarkably enriched in the anti-Ago2 group relative to the anti-immunoglobulin G (IgG) group (Figure 3F), demonstrating that both of them existed in the Ago2-composed RNA-induced silencing complex (RISC).

Given that DKK1 is a well-accepted inhibitor of the Wnt/β-catenin pathway that contributes a lot to lung cancer progression,[23–25] we then detected the influence of circ_0018414 on the Wnt/β-catenin pathway. The results of western blot disclosed that the levels of several related proteins, including c-*myc*, cyclin D1, and β-catenin, were all inhibited along with the enhanced DKK1 level resulting from circ_0018414 upregulation (Figure 3G). Consistently, upregulating circ_0018414 in LUAD cells restrained the luciferase activity of the TOP vector while that of the FOP vector exhibited no apparent changes (Figure 3H). The reduced TOP/FOP ratio meant declined activity of the Wnt/β-catenin pathway in circ_0018414-overexpressed LUAD cells. Additionally, the outcomes of sphere-formation assays revealed that the sphere formation ability of LUAD cells was impaired in face of circ_0018414 overexpression (Figure 3I). In addition, we also detected that the expression of stemness-related proteins (OCT4, SOX2, and Nanog) declined in response to circ_0018414 overexpression (Figure 3J). All in all, circ_0018414 could positively regulate DKK1 expression to inactivate the Wnt/β-catenin signaling pathway in LUAD cells.

circ_0018414 sponged miR-6807-3p

Then, we probed into the miRNA that linked circ_0018414 to DKK1 in LUAD cells. Based on the starBase database (http://starbase.sysu.edu.cn/), there were 38 candidate miRNAs that were not only sponged by circ_0018414 but also targeted DKK1 (Figure 4A). Among them, only miR-2682-5p, miR-500b-5p, miR-664b-3p, and miR-6807-3p were previously reported to be anti-tumor genes, which were further focused on subsequently. Thereafter, the results of the circRNA *in vivo* precipitation (circRIP) assay demonstrated that only miR-6807-3p was significantly pulled down by biotinylated circ_0018414 (Figure 4B). Moreover, miR-6807-3p expression was extraordinarily high in LUAD tissues compared to adjacent non-tumor tissues (Figure 4C). Also, miR-6807-3p had a negative correlation with circ_0018414 in expression in LUAD tissues (Figure 4D). Intriguingly, overexpressing circ_0018414 had no impact on the expression of miR-6807-3p, whereas ectopic expression of miR-6807-3p evidently lessened circ_0018414 levels in LUAD cells (Figure S1G). The predicted binding site between circ_0018414 and miR-6807-3p is presented in Figure 4E. Next, miR-6807-3p was silenced in LUAD cells by transfection of the miR-6807-3p inhibitor (Figure 4F). Afterward, depletion of miR-6807-3p led to enhanced luciferase activity of wild-type (WT) circ_0018414, but it exerted no influence on that of mutant (Mut) circ_0018414 (Figure 4G). Such phenomena indicated that circ_0018414 bound with miR-6807-3p at the predicted site. Subsequently, the function of miR-6807-3p in LUAD was further probed. The data from CCK-8 assays and colony formation experiments unveiled that miR-6807-3p downregulation hindered LUAD cell proliferation (Figures 4H and 4I). However, the apoptosis of LUAD cells was promoted as a result of miR-6807-3p deficiency (Figure 4J). In conclusion, miR-6807-3p was sponged by circ_0018414, and inhibiting miR-6807-3p restrained LUAD progression.

miR-6807-3p targeted DKK1 to activate the Wnt/β-catenin pathway

Furthermore, we probed the relationship between miR-6807-3p and DKK1 in LUAD cells. Before that, we discovered three potential binding sites for miR-6807-3p in the DKK1 3′ UTR (Figure S1H). Efficient upregulation of miR-6807-3p was validated in LUAD cells according to the data from quantitative real-time PCR (Figure 5A). Then, a luciferase reporter experiment was implemented in HEK293T cells to validate the precise site responsible for the binding of miR-6807-3p to DKK1. Results showed that the luciferase activity of WT DKK1 was reduced by upregulation of miR-6807-3p, while such reduction was gradually reversed when the predicted three sites were successively mutated (Figure S1I), which indicated that all the three sites in the DKK1 3′ UTR were recognized by miR-6807-3p. Also, we verified that upregulating miR-6807-3p had a suppressive impact on the luciferase activity of WT DKK1 but not Mut DKK1 in LUAD cells (Figure 5B), while such an effect was restored due to circ_0018414 overexpression (Figure 5C). Moreover, miR-6807-3p upregulation triggered the downregulation of DKK1, leading to elevated levels of c-*myc*, cyclin D1, and β-catenin in LUAD cells (Figures 5D and 5E). On the contrary, miR-6807-3p inhibition in LUAD cells resulted in opposite phenomena (Figure 5F). As expected, changes in miR-6807-3p expression had no impact on DKK1 precursor (pre-)mRNA (Figure S2A). These data proved that miR-6807-3p regulated DKK1 at the post-transcriptional level but not at the transcriptional level.

Subsequently, we examined whether circ_0018414 affected the Wnt/β-catenin pathway through a miR-6807-3p-mediated manner. The results showed that the effects of circ_0018414 overexpression on the protein levels of c-*myc*, cyclin D1, β-catenin, and DKK1 were

Figure 2. circ_0018414 served as an anti-oncogene in LUAD cells

(A) The expression of circ_0018414 in A549 and SPC-A1 cells transfected with empty vector or circ_0018414 overexpression vector was detected by quantitative real-time PCR. Unpaired Student's t test. (B) CCK-8 assay evaluated the proliferation ability of LUAD cells with or without overexpression of circ_0018414. Two-way ANOVA. (C and D) Colony formation and EdU assays (scale bars, 120 μm) tested the effect of circ_0018414 upregulation on LUAD cell proliferation. Unpaired Student's t test. (E and F) Flow cytometry analysis and TUNEL assay (scale bars, 120 μm) illustrated the impact of circ_0018414 upregulation on cell apoptosis in LUAD. Unpaired Student's t test. (G) JC-1 staining assays (scale bars, 40 μm) detected the changes in mitochondrial membrane potential in LUAD cells after circ_0018414 upregulation. Unpaired Student's t test. $^{**}p < 0.01$. Error bars indicate SD; n = 5 in each experiment.

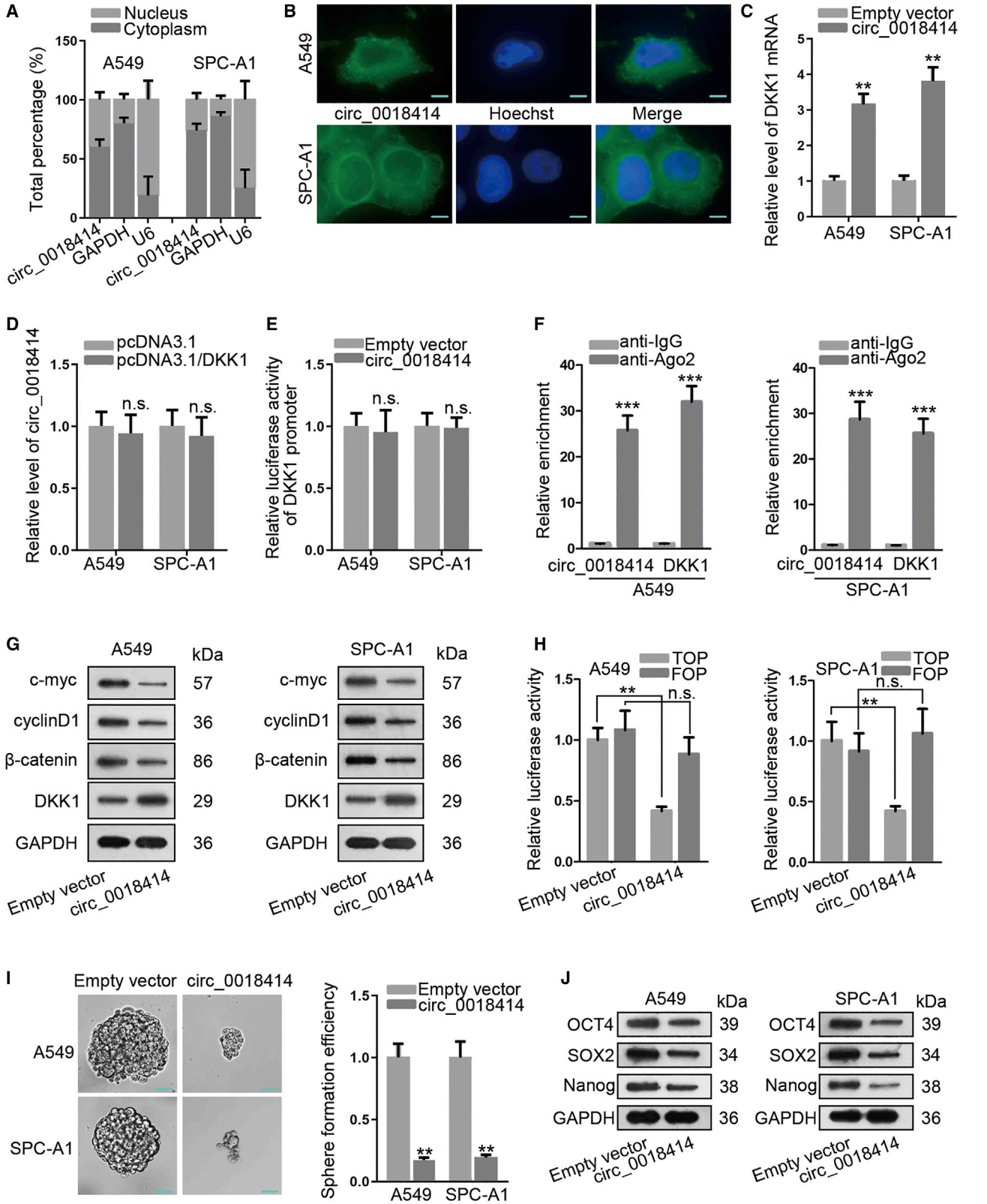

(legend on next page)

offset after co-transfection with miR-6807-3p mimics (Figure S2B). More interestingly, luciferase activity of the TOP vector was increased because of miR-6807-3p upregulation, but that of the FOP vector disclosed no change (Figure 5G). The elevated TOP/FOP ratio implied that overexpression of miR-6807-3p activated the Wnt/β-catenin pathway in LUAD cells. After that, we upregulated DKK1 expression in LUAD cells, and the overexpression efficiency of DKK1 was verified through quantitative real-time PCR and western blot analyses (Figure S2C). As shown by the data from cell proliferation assays, overexpression of DKK1 markedly inhibited the proliferation of LUAD cells (Figures S2D and S2E). Additionally, the apoptosis rate was overtly enhanced in LUAD cells in response to DKK1 upregulation (Figure S2F). In general, miR-6807-3p targeted DKK1 to activate the Wnt/β-catenin pathway in LUAD cells.

circ_0018414 inhibited LUAD progression by modulating the miR-6807-3p/DKK1 axis to inactivate the Wnt/β-catenin pathway

Finally, rescue assays were conducted in circ_0018414-overexpressed A549 cells to confirm whether circ_0018414 hindered LUAD progression through the miR-6807-3p/DKK1 axis to inactivate the Wnt/β-catenin pathway. The outcomes of cell proliferation experiments showed that DKK1 overexpression could reverse the promoting influence of miR-6807-3p upregulation on cell proliferation, while by LiCl treatment, this effect was abolished (Figures 6A–6C). Meanwhile, flow cytometry analysis and JC-1 assay data illustrated that DKK1 overexpression could recover the stimulating effect of miR-6807-3p overexpression on cell apoptosis, while under LiCl treatment, this effect was reversed (Figures 6D and 6E). We then performed *in vivo* assays to further probe into the function of circ_0018414 in LUAD. It was revealed that tumor size, volume, and weight were decreased as a result of circ_0018414 upregulation, while the recovery of these aspects was observed in tumors with further overexpression of miR-6807-3p (Figures 6F–6H). Consistently, the attenuated expression of the cell proliferation marker Ki67 and the enhanced expression of DKK1 owing to circ_0018414 overexpression in these xenografts were both reversed by ectopic expression of miR-6807-3p (Figure 6I). These data suggested that circ_0018414 depended on miR-6807-3p to block tumor growth in LUAD.

All in all, circ_0018414 inhibited the progression of LUAD via serving as a sponge of miR-6807-3p to upregulate DKK1 and therefore inactivate the Wnt/β-catenin pathway.

DISCUSSION

Previous reports have revealed that circRNAs contribute to the progression of several cancers, including LUAD. For example, circMTO1 suppresses the proliferation of LUAD cells via regulating the miR-17/QKI-5 pathway.[26] circRNA circ_0005962 is upregulated in LUAD and promotes proliferation of LUAD cells.[27] circRNA hsa_circ_0006427 inhibits LUAD development via sponging miR-6783-3p and upregulating DKK1 to inactivate the Wnt/β-catenin pathway.[19] circ_0000792 expression is boosted in LUAD tissues and it modulates LUAD progression via sponging miR-375.[28] The present study revealed that circ_0018414 was significantly downregulated in LUAD tissues and cells. Moreover, circ_0018414 expression had a positive connection with the prognosis of LUAD patients. Functionally, circ_0018414 overexpression alleviated cell proliferation and stemness while it promoted cell apoptosis in LUAD. Also, *in vivo* assays illustrated that circ_0018414 overexpression hindered tumor growth in LUAD.

DKK1 is the host gene of circ_0018414, which is a well-known suppressor of the Wnt/β-catenin pathway. Functionally, DKK1 could bind to Wnt co-receptor-related protein-5/6 (LRP5/6) to hinder activation of the Wnt/β-catenin pathway.[29] Increasing evidence has shown that DKK1 plays vital roles in cancers. For example, upregulation of DKK1 represses cell proliferation, migration, and invasion, but it boosts cell apoptosis in colorectal cancer.[30] Of note, DKK1 is proved to hinder cell proliferation and migration by inactivating the Wnt/β-catenin pathway in LUAD.[19] Our study established that DKK1 was positively regulated by circ_0018414 at both the mRNA and protein levels. Also, DKK1 overexpression could repress cell proliferation but facilitate cell apoptosis in LUAD. In addition, DKK1 upregulation suppressed the Wnt/β-catenin pathway.

miRNAs are a subtype of non-coding RNAs with 20–22 nt, and they can post-transcriptionally modulate target genes through RISC.[31] In terms of mechanism, circRNAs can sponge specific miRNAs to modulate the expression of genes.[32–34] In present study, circ_0018414 was confirmed to locate in the cytoplasm and sponge miR-6807-3p in LUAD cells. Also, miR-6807-3p was confirmed to target DKK1. Moreover, miR-6807-3p overexpression could boost cell proliferation and suppress cell apoptosis in LUAD.

In summary, the present research confirmed that circ_0018414 blocked the progression of LUAD via sponging miR-6807-3p and

Figure 3. circ_0018414 positively regulated DKK1 expression to inactivate Wnt/β-catenin signaling pathway

(A and B) Subcellular fractionation assay and RNA FISH assay (scale bars, 20 μm) examined the distribution of circ_0018414 in LUAD cells. (C) Quantitative real-time PCR examined the mRNA expression of DKK1 in LUAD cells under overexpression of circ_0018414. Unpaired Student's t test. (D) Quantitative real-time PCR evaluated the influence of DKK1 on the expression of circ_0018414 in LUAD cells. Unpaired Student's t test. (E) Luciferase reporter assay analyzed the luciferase activity of the DKK1 promoter in LUAD cells with or without circ_0018414 overexpression. Unpaired Student's t test. (F) RIP assay tested the enrichment of circ_0018414 and DKK1 in anti-Ago2 groups relative to anti-IgG groups. Unpaired Student's t test. (G) Western blot analyzed the level of the Wnt/β-catenin signaling pathway-related proteins (c-*myc*, cyclin D1, and β-catenin) and DKK1 in LUAD cells under circ_0018414 overexpression. (H) TOP/FOP Flash luciferase reporter assay tested the activity of Wnt/β-catenin signaling in LUAD cells with overexpression of circ_0018414. One-way ANOVA. (I) Sphere-formation assays (scale bars, 150 μm) detected the stemness of LUAD cells with or without overexpression of circ_0018414. Unpaired Student's t test. (J) Western blot determined the expression of stemness-related proteins (OCT4, SOX2, and Nanog) in LUAD cells under circ_0018414 upregulation. $^{**}p < 0.01$, $^{***}p < 0.001$. n.s., not significant. Error bars indicate SD; n = 5 in each experiment.

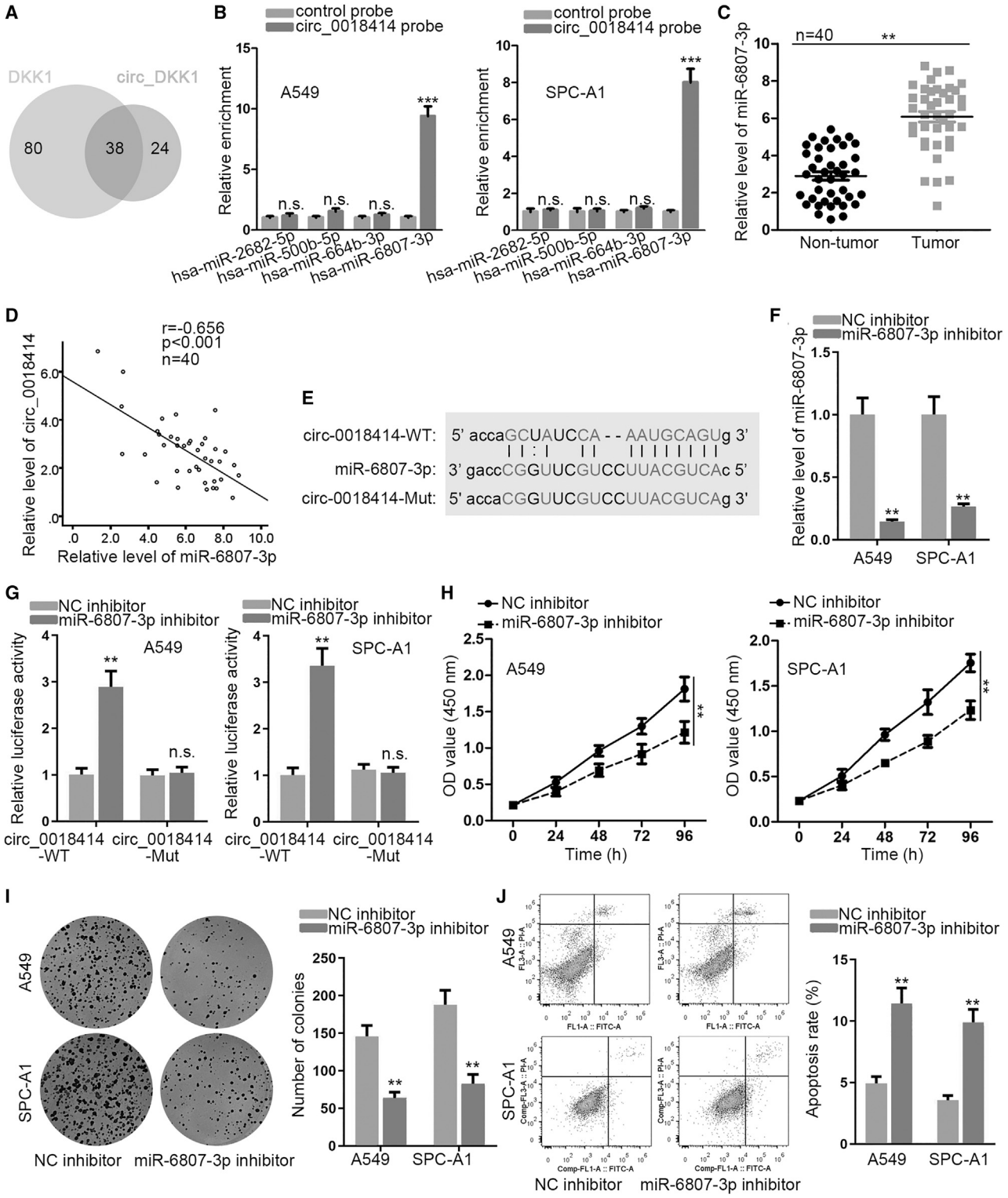

Figure 4. circ_0018414 sponged miR-6807-3p

(A) starBase predicted miRNAs that could interact with circ_0018414 and DKK1. (B) circRIP detected the interaction between circ0018414 and indicated miRNAs. Unpaired Student's t test. (C) Quantitative real-time PCR analyzed miR-6807-3p expression in LUAD tissues and matched non-tumor tissues. Paired Student's t test. (D) Pearson's

(legend continued on next page)

upregulating DKK1 to inactivate the Wnt/β-catenin pathway. This discovery might make a difference for the treatment of LUAD in the future.

MATERIALS AND METHODS

Tissue samples

LUAD tissues and paired non-tumor tissues used in current study were obtained from LUAD patients in Hwa Mei Hospital, University of Chinese Academy of Sciences (Ningbo No. 2 Hospital). All participants only received surgical treatment and provided informed consent before operation. Our study conformed to the standards set by the Declaration of Helsinki and was approved by the Ethics Committee of Hwa Mei Hospital, University of Chinese Academy of Sciences (Ningbo No. 2 Hospital). Samples were immediately frozen in liquid nitrogen and stored at 80°C before use.

Cell culture

Human LUAD cell lines (H1299, A549, SPC-A1, and Calu3) and normal human lung epithelial cell line HBE were provided by the Institute of Cell Research, Chinese Academy of Sciences (Shanghai, China). All cell lines were maintained in Dulbecco's modified Eagle's medium (DMEM; Invitrogen, Carlsbad, CA, USA) consisting of 10% fetal bovine serum (FBS, Gibco, Carlsbad, USA), 100 U/mL penicillin, and 100 μg/mL streptomycin (Invitrogen) with 5% CO_2 at 37°C.

Cell transfection

The sequence of circ_0018414 was inserted into the PLCDH-cir vector (Ribobio, Guangzhou, China) to produce lentivirus for circ_0018414 overexpression. Short hairpin RNA (shRNA) targeting circ_0018414 (sh-circ_0018414) was applied for downregulating circ_0018414. In order to upregulate DKK1, the full-length of the DKK1 cDNA sequence was cloned into the pcDNA3.1 vector (GenePharma, Shanghai, China). miR-6807-3p mimics/inhibitor were gained from GenePharma, with negative control (NC) mimics/inhibitor as corresponding NCs. All of the plasmids were transfected into LUAD cells by the use of Lipofectamine 3000 (Invitrogen).

RNA extraction, quantitative real-time PCR, and RNase R treatment

Total RNA was extracted from LUAD tissues and cells with TRIzol reagent (Invitrogen). Reverse transcription was implemented with a PrimeScript RT kit (Takara, Dalian, China) to produce the first-strand complementary DNA (cDNA). miR-6807-3p was reverse transcribed with a TaqMan advanced miRNA cDNA synthesis kit (Takara). Quantitative real-time PCR was performed using SYBR Green (Applied Biosystems, Foster City, CA, USA). circ_0018414, miR-6807-3p, and DKK1 expression levels were counted by the $2^{-\Delta\Delta Ct}$ method, with GAPDH and U6 as the internal controls as needed.

For RNase R treatment, 2 mg of total RNA was incubated with 3 U/mg RNase R (Epicenter Technologies, Madison, WI, USA) for 15 min at 37°C. The group without RNase R treatment served as the mock. The levels of circ_0018414, DKK1, and GAPDH in both groups were evaluated by quantitative real-time PCR.

JC-1 staining

A549 and SPC-A1 cells were plated on 60-mm dishes and then incubated for one night. Then, cells were treated with the compounds in a fresh medium including 5% bovine growth serum. After the dishes were washed twice with PBS for 2 h, the fluorescence of JC-1 was examined through a Becton Dickinson FACSCalibur analytical flow cytometer (BD Biosciences, San Jose, CA, USA). Subsequently, the JC-1 ratio of red fluorescence (530 nm) to green fluorescence (590 nm) was counted.

Sphere-formation assay

A sphere-formation assay was implemented as described.[35] A549 or SPC-A1 cells were seeded in six-well plates (Corning Life Sciences, Kraemer, CA, USA). Then, cells were processed with serum-free DMEM, which contained 20 mg/L epidermal growth factor (EGF), 20 mg/L human fibroblast growth factor (hFGF), 4 U/L insulin, and 100 U/mL penicillin/streptomycin. Finally, spheroids were calculated under a stereomicroscope (Olympus, Tokyo, Japan).

CCK-8 assay

To investigate the proliferation ability of LUAD cells, an assay was performed by use of a CCK-8 kit (Solarbio, China) as per the manufacturer's guide. In brief, cells were planted into 96-well plates for one night. Furthermore, after 0, 24, 48, 72, or 96 h of incubation, 10 μL of CCK-8 solution was supplemented into each well. Finally, the absorbance value (450 nm) was determined with a microplate reader.

Colony formation assay

Cells were inoculated into six-well plates and then cultured in DMEM supplied with 10% FBS. After incubation for 14 days, methanol was used to fix the colonies followed by the staining of colonies with 1% crystal violet. At last, colonies with no less than 50 cells were counted manually.

EdU assay

Cells were cultured into 24-well plates and then an EdU reagent was added into each well. After incubation, cells were fixed with 4%

correlation analysis determined the expression correlation of miR-6807-3p with circ_0018414 in LUAD tissues. (E) The binding site between circ_0018414 and miR-6807-3p predicted by starBase is presented. (F) Quantitative real-time PCR tested miR-6807-3p expression in LUAD cells. Unpaired Student's t test. (G) Luciferase reporter assay tested the impact of miR-6807-3p inhibition on the luciferase activity of circ_0018414-WT/Mut. Unpaired Student's t test. (H and I) CCK-8 (two-way ANOVA) and colony formation assays (Unpaired Student's t test) detected the proliferation of LUAD cells with or without miR-6807-3p overexpression. (J) Flow cytometry analyzed the influence of miR-6807-3p overexpression on cell apoptosis in LUAD. Unpaired Student's t test. $^{**}p < 0.01$, $^{***}p < 0.001$. n.s., not significant. Error bars indicate SD; n = 5 in each experiment.

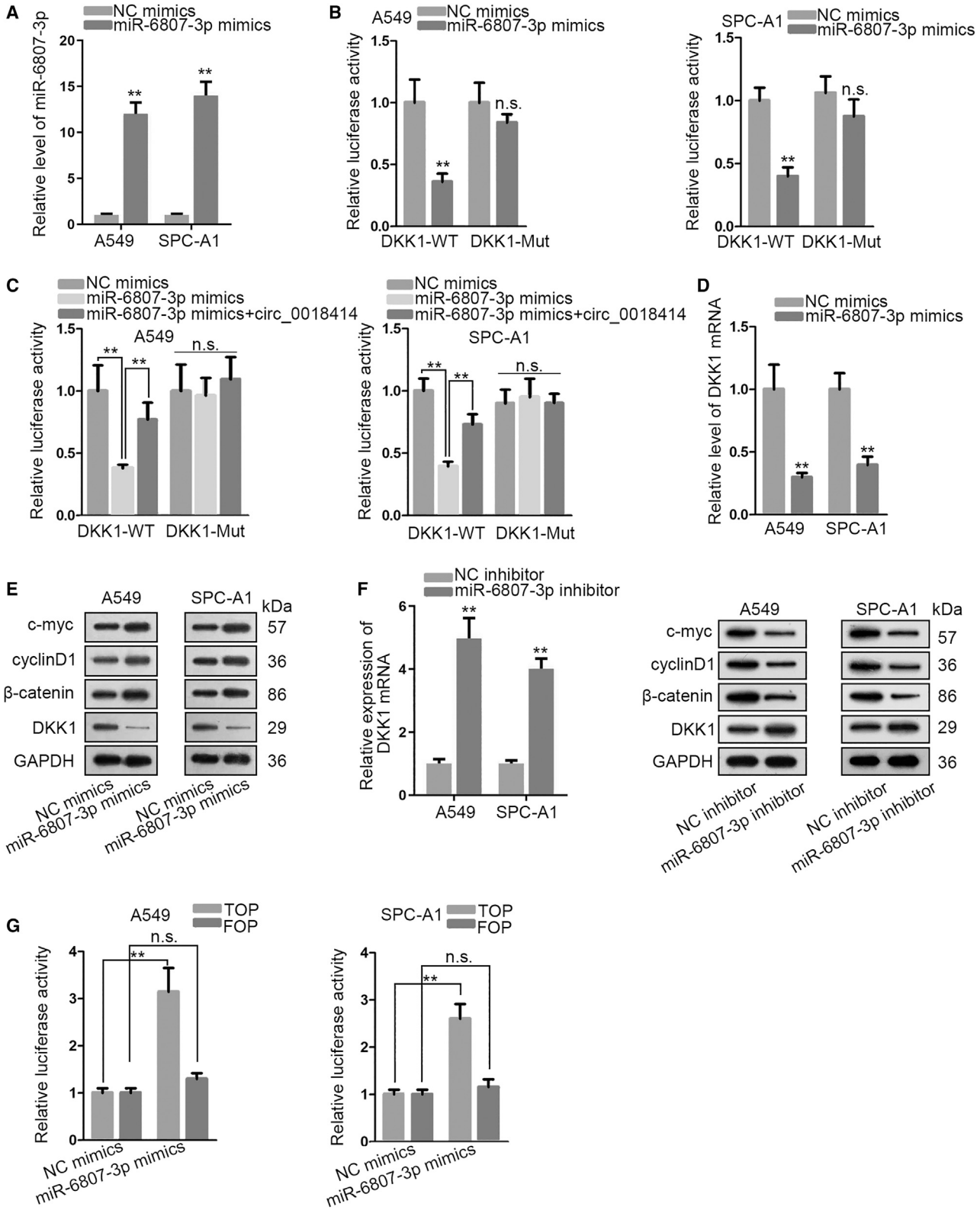

(legend on next page)

formaldehyde. After that, an EdU labeling and detection kit (Ribobio, Guangzhou, China) was used to stain proliferative cells. Following nuclei staining via DAPI (Invitrogen, CA, USA), cells were analyzed under a microscope.

TUNEL assay

For assessing cell apoptosis, a TUNEL assay was implemented with an *in situ* cell death detection kit (Roche). Transfected A549 and SPC-A1 cells were treated with 10 nmol/L DTX. Thereafter, cells were washed and stained by TUNEL and DAPI. In the end, TUNEL-stained cells were counted under a fluorescence microscope (Zeiss, Oberkochen, Germany).

Western blot analysis

Radioimmunoprecipitation assay (RIPA) buffer was utilized for extracting total proteins. Then, the proteins were isolated with 10% sodium dodecyl sulfate-polyacrylamide gel electrophoresis (SDS-PAGE) and subsequently transferred to polyvinylidene fluoride (PVDF) membranes (Millipore, Billerica, MA, USA). After that, membranes were blocked with 5% nonfat milk and then cultured with primary antibodies at 4°C overnight. The primary antibodies were purchased from Abcam (Cambridge, UK), including anti-c-*myc*, anti-cyclin D1, anti-β-catenin, anti-DKK1, anti-OCT4, anti-SOX2, anti-Nanog, and anti-GAPDH. Next, the membranes were processed with secondary antibodies at indoor temperature for 1 h. GAPDH served as the internal control. Through using the enhanced chemiluminescence (ECL) detection kit (Millipore), the protein signals were visualized.

Flow cytometry analysis

Flow cytometry analysis was carried out for determining cell apoptosis rate. Through a fluorescein isothiocyanate (FITC) annexin V apoptosis detection kit (Ruibo, Guangzhou, China), cells were stained and then the apoptosis rate was detected with flow cytometry (Becton Dickinson, Mountain View, CA, USA).

FISH

Cells were fixed in 4% paraformaldehyde and washed with PBS for 30 min. After treating with FISH probes specific for circ_0018414 in hybridization buffer overnight, cells were washed with PBS three times and then blocked with HRP blocker. Afterward, Hoechst was used to counterstain cell nuclei. Finally, an FV10i confocal microscope (Olympus, Tokyo, Japan) was utilized to observe cells in the slides.

Subcellular fractionation assay

The separation of cell cytoplasm and nucleus was accomplished with a Paris kit (Invitrogen). First, A549 and SPC-A1 cells were lysed in cell fractionation buffer and were centrifuged. RNAs isolated from nuclear and cytoplasmic extracts were collected by applying TRIzol (Life Technologies, Carlsbad, CA, USA) and then analyzed via quantitative real-time PCR. GAPDH was used as cytoplasmic control while U6 was used as nuclear control.

circRIP assay

The circRIP assay was implemented to examine the association between circ_0018414 and candidate 4 miRNAs. Cells were fixed with formaldehyde and then sonicated. After that, the supernatant was cultured with the magnetic streptavidin Dynabeads that were precoated with the biotinylated circ_0018414 probe. After total RNA was extracted, the enrichment of indicated miRNAs was subjected to quantitative real-time PCR analysis.

Luciferase reporter assay

The Dual-Luciferase reporter assay system (Promega, Fitchburg, WI, USA) was applied for this experiment. The sequence of full-length circ_0018414/DKK1 3′UTR with WT or Mut binding sites for miR-6807-3p was inserted into pmirGLO vector (Promega, Madison, WI, USA). Then, pmirGLO-circ_0018414-WT/Mut plasmids (or pmirGLO-DKK1-WT/Mut plasmids) were co-transfected with indicated transfection plasmids into LUAD cells. After transfection for 48 h, the luciferase activity normalized to Renilla luciferase activity was analyzed via a Dual-Luciferase reporter assay system.

TOP/FOP Flash assay

TOP Flash luciferase reporter vector (with a TCF/LEF DNA binding site) and FOP Flash luciferase reporter vector (with a Mut TCF/LEF DNA binding site) were obtained from Biovector NTCC (Beijing, China). Briefly, cells in 96-well plates were co-transfected with TOP Flash (or FOP Flash) and circ_0018414 overexpression vector (or empty vector) or miR-6807-3p mimics (or NC mimics). Relative luciferase activity of TOP/FOP Flash was determined by the firefly luciferase activity after normalizing to respective Renilla luciferase activity. The ratio of TOP Flash luciferase activity to FOP Flash luciferase activity was used to indicate the activity of the Wnt/β-catenin pathway.

In vivo xenograft experiments

The Animal Research Committee of Hwa Mei Hospital, University of Chinese Academy of Sciences (Ningbo No.2 Hospital),

Figure 5. miR-6807-3p targeted DKK1 to activate the Wnt/β-catenin pathway in LUAD cells

(A) Quantitative real-time PCR tested miR-6807-3p expression in LUAD cells transfected with NC mimics or miR-6807-3p mimics. Unpaired Student's t test. (B) Luciferase reporter assay tested the impact of miR-6807-3p overexpression on the luciferase activity of DKK1-WT/Mut. Unpaired Student's t test. (C) Luciferase reporter assay manifested the luciferase activity of DKK1-WT/Mut in LUAD cells under different transfections. One-way ANOVA. (D) Quantitative real-time PCR tested DKK1 expression in LUAD cells under miR-6807-3p overexpression. Unpaired Student's t test. (E) Western blot analyzed the protein levels of c-*myc*, cyclin D1, β-catenin, and DKK1 in LUAD cells with or without miR-6807-3p overexpression. (F) Quantitative real-time PCR analyzed DKK1 mRNA expression and western blot analyzed the levels of proteins related to Wnt/β-catenin pathway in indicated LUAD cells. Unpaired Student's t test. (G) TOP/FOP flash luciferase reporter assay detected changes in the activity of the Wnt/β-catenin pathway in LUAD cells after miR-6807-3p overexpression. One-way ANOVA. $^{**}p < 0.01$. n.s., not significant. Error bars indicated SD; n = 5 in each experiment.

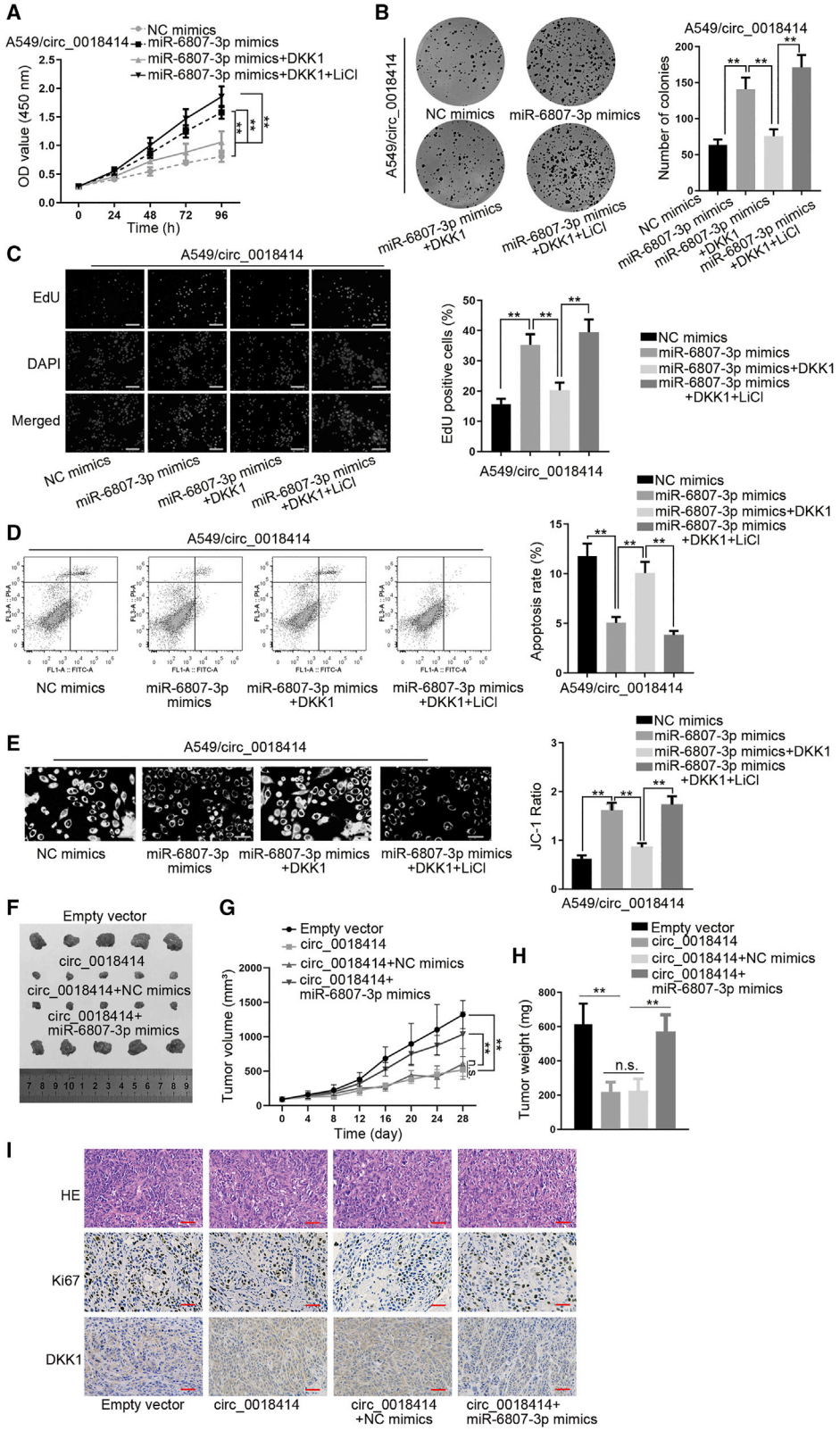

(legend on next page)

approved the protocols for animal experiments. The mice (4-week-old BALB/c nude female mice, five per group) were subcutaneously injected with indicated A549 cells, and every 4 days the tumor volume was recorded. The mice were all sacrificed at day 28 and tumor tissues were collected for weight measurement and other analysis.

Immunohistochemistry (IHC)

After fixing in 10% formalin solution, xenograft samples were embedded in paraffin and then sliced into sections. Thereafter, the sections were cultured with antibody specific to Ki67 (Abcam, Boston, MA, USA) or DKK1 (Abcam), followed by further incubation with the secondary antibodies (Thermo Fisher Scientific, Waltham, MA, USA). Finally, the images were visualized under an Olympus microscope.

RIP assay

A Magna RIP RNA-binding protein immunoprecipitation kit (Millipore, Billerica, MA, USA) was used for the RIP assay. LUAD cells were lysed in RIP lysis buffer. Then, cell lysates were cultured with RIP buffer containing magnetic beads that were pre-coated with Ago2 antibodies (Abcam) or IgG antibodies at 4°C overnight. Finally, the immunoprecipitated RNA was purified and quantified by quantitative real-time PCR.

Statistical analysis

Data analyses were carried out using SPSS version 16.0 software (IBM, Chicago, IL, USA). The data were presented as the means ± standard deviation (SD) from at least three independent assays. Comparisons between two groups were analyzed by a paired or unpaired Student t test. One-way or two-way analysis of variance (ANOVA) was used for comparisons among multiple groups. Overall survival (OS) of LUAD patients with a high or low level of circ_0018414 was assessed with the Kaplan-Meier analysis and log-rank test. The correlation between circ_0018414 and miR-6807-3p was tested using Pearson's correlation analysis. Statistical significance was determined by a p value less than 0.05.

SUPPLEMENTAL INFORMATION

Supplemental Information can be found online at https://doi.org/10.1016/j.omtn.2020.12.031.

ACKNOWLEDGMENTS

We appreciate the support of all of our lab members.

AUTHOR CONTRIBUTIONS

Y.Y. performed all of the experiments, analyzed the data, and wrote the manuscript; Y.Z. and Q.H. reviewed and edited the manuscript; Y.Y. is the guarantor of this work, had full access to all of the data in the study, and takes responsibility for the integrity of the data and the accuracy of the data analysis.

DECLARATION OF INTERESTS

The authors declare no competing interests.

REFERENCES

1. Torre, L.A., Siegel, R.L., and Jemal, A. (2016). Lung cancer statistics. Adv. Exp. Med. Biol. *893*, 1–19.
2. Wu, C., Xu, B., Zhou, Y., Ji, M., Zhang, D., Jiang, J., and Wu, C. (2016). Correlation between serum IL-1β and miR-144-3p as well as their prognostic values in LUAD and LUSC patients. Oncotarget *7*, 85876–85887.
3. Yan, L., Jiao, D., Hu, H., Wang, J., Tang, X., Chen, J., and Chen, Q. (2017). Identification of lymph node metastasis-related microRNAs in lung adenocarcinoma and analysis of the underlying mechanisms using a bioinformatics approach. Exp. Biol. Med. (Maywood) *242*, 709–717.
4. Wu, K., House, L., Liu, W., and Cho, W.C. (2012). Personalized targeted therapy for lung cancer. Int. J. Mol. Sci. *13*, 11471–11496.
5. Yang, F., Zhu, P., Guo, J., Liu, X., Wang, S., Wang, G., Liu, W., Wang, S., and Ge, N. (2017). Circular RNAs in thoracic diseases. J. Thorac. Dis. *9*, 5382–5389.
6. Sanger, H.L., Klotz, G., Riesner, D., Gross, H.J., and Kleinschmidt, A.K. (1976). Viroids are single-stranded covalently closed circular RNA molecules existing as highly base-paired rod-like structures. Proc. Natl. Acad. Sci. USA *73*, 3852–3856.
7. Jeck, W.R., and Sharpless, N.E. (2014). Detecting and characterizing circular RNAs. Nat. Biotechnol. *32*, 453–461.
8. Bi, W., Huang, J., Nie, C., Liu, B., He, G., Han, J., Pang, R., Ding, Z., Xu, J., and Zhang, J. (2018). circRNA circRNA_102171 promotes papillary thyroid cancer progression through modulating CTNNBIP1-dependent activation of β-catenin pathway. J. Exp. Clin. Cancer Res. *37*, 275.
9. Huang, X.Y., Huang, Z.L., Zhang, P.B., Huang, X.Y., Huang, J., Wang, H.C., Xu, B., Zhou, J., and Tang, Z.Y. (2019). circRNA-100338 is associated with mTOR signaling pathway and poor prognosis in hepatocellular carcinoma. Front. Oncol. *9*, 392.
10. Zhou, X., Natino, D., Qin, Z., Wang, D., Tian, Z., Cai, X., Wang, B., and He, X. (2017). Identification and functional characterization of circRNA-0008717 as an oncogene in osteosarcoma through sponging miR-203. Oncotarget *9*, 22288–22300.
11. Zhang, Y., Liu, H., Li, W., Yu, J., Li, J., Shen, Z., Ye, G., Qi, X., and Li, G. (2017). circRNA_100269 is downregulated in gastric cancer and suppresses tumor cell growth by targeting miR-630. Aging (Albany NY) *9*, 1585–1594.
12. Huang, G., Li, S., Yang, N., Zou, Y., Zheng, D., and Xiao, T. (2017). Recent progress in circular RNAs in human cancers. Cancer Lett. *404*, 8–18.
13. Cheng, Z., Yu, C., Cui, S., Wang, H., Jin, H., Wang, C., Li, B., Qin, M., Yang, C., He, J., et al. (2019). *circTP63* functions as a ceRNA to promote lung squamous cell carcinoma progression by upregulating FOXM1. Nat. Commun. *10*, 3200.
14. Yu, J., Yang, M., Zhou, B., Luo, J., Zhang, Z., Zhang, W., and Yan, Z. (2019). circRNA-104718 acts as competing endogenous RNA and promotes hepatocellular carcinoma

Figure 6. circ_0018414 inhibited the progression of LUAD by sponging miR-6807-3p and upregulating DKK1 to inactivate the Wnt/β-catenin signaling pathway

(A–C) CCK-8 (two-way ANOVA), colony formation (one-way ANOVA), and EdU assays (one-way ANOVA) (scale bars, 120 μm) detected LUAD cell proliferation ability under different conditions. (D and E) Flow cytometry analysis and JC-1 staining assay (scale bars, 40 μm) disclosed LUAD cell apoptosis ability under different conditions. One-way ANOVA. (F–H) Representative images, growth curve (two-way ANOVA), and weight (one-way ANOVA) of tumors obtained from different groups of *in vivo* experiment. (I) IHC assay (scale bars, 150 μm) analyzed Ki67 and DKK1 expression in tumors obtained from indicated groups. $^{**}p < 0.01$. n.s., not significant. Error bars indicate SD; n = 5 in each experiment.

progression through microRNA-218-5p/TXNDC5 signaling pathway. Clin. Sci. (Lond.) *133*, 1487–1503.

15. Sang, Y., Chen, B., Song, X., Li, Y., Liang, Y., Han, D., Zhang, N., Zhang, H., Liu, Y., Chen, T., et al. (2019). circRNA_0025202 regulates tamoxifen sensitivity and tumor progression via regulating the miR-182-5p/FOXO3a axis in breast cancer. Mol. Ther. *27*, 1638–1652.
16. Shi, Y., Guo, Z., Fang, N., Jiang, W., Fan, Y., He, Y., Ma, Z., and Chen, Y. (2019). hsa_-circ_0006168 sponges miR-100 and regulates mTOR to promote the proliferation, migration and invasion of esophageal squamous cell carcinoma. Biomedicine Pharmacother *117*, 109151.
17. Sheng, M., Wei, N., Yang, H.Y., Yan, M., Zhao, Q.X., and Jing, L.J. (2019). circRNA UBAP2 promotes the progression of ovarian cancer by sponging microRNA-144. Eur. Rev. Med. Pharmacol. Sci. *23*, 7283–7294.
18. Yao, Y., Hua, Q., Zhou, Y., and Shen, H. (2019). circRNA has_circ_0001946 promotes cell growth in lung adenocarcinoma by regulating miR-135a-5p/SIRT1 axis and activating Wnt/β-catenin signaling pathway. Biomed. Pharmacother *111*, 1367–1375.
19. Yao, Y., Hua, Q., and Zhou, Y. (2019). circRNA has_circ_0006427 suppresses the progression of lung adenocarcinoma by regulating miR-6783-3p/DKK1 axis and inactivating Wnt/β-catenin signaling pathway. Biochem. Biophys. Res. Commun. *508*, 37–45.
20. Niu, J., Li, X.M., Wang, X., Liang, C., Zhang, Y.D., Li, H.Y., Liu, F.Y., Sun, H., Xie, S.Q., and Fang, D. (2019). DKK1 inhibits breast cancer cell migration and invasion through suppression of β-catenin/MMP7 signaling pathway. Cancer Cell Int. *19*, 168.
21. Wang, C., Tan, C., Wen, Y., Zhang, D., Li, G., Chang, L., Su, J., and Wang, X. (2019). FOXP1-induced lncRNA CLRN1-AS1 acts as a tumor suppressor in pituitary prolactinoma by repressing the autophagy via inactivating Wnt/β-catenin signaling pathway. Cell Death Dis. *10*, 499.
22. Yang, J., Liu, Y., Mai, X., Lu, S., Jin, L., and Tai, X. (2019). STAT1-induced upregulation of LINC00467 promotes the proliferation migration of lung adenocarcinoma cells by epigenetically silencing DKK1 to activate Wnt/β-catenin signaling pathway. Biochem. Biophys. Res. Commun. *514*, 118–126.
23. Wang, Z., Yang, M.Q., Lei, L., Fei, L.R., Zheng, Y.W., Huang, W.J., Li, Z.H., Liu, C.C., and Xu, H.T. (2019). Overexpression of KRT17 promotes proliferation and invasion of non-small cell lung cancer and indicates poor prognosis. Cancer Manag. Res. *11*, 7485–7497.
24. Yang, Y., Li, Z., Yuan, H., Ji, W., Wang, K., Lu, T., Yu, Y., Zeng, Q., Li, F., Xia, W., and Lu, S. (2019). Reciprocal regulatory mechanism between miR-214-3p and FGFR1 in FGFR1-amplified lung cancer. Oncogenesis *8*, 50.
25. Cui, J., Pan, G., He, Q., Yin, L., Guo, R., and Bi, H. (2019). MicroRNA-545 targets ZEB2 to inhibit the development of non-small cell lung cancer by inactivating Wnt/β-catenin pathway. Oncol. Lett. *18*, 2931–2938.
26. Zhang, B., Chen, M., Jiang, N., Shi, K., and Qian, R. (2019). A regulatory circuit of circ-MTO1/miR-17/QKI-5 inhibits the proliferation of lung adenocarcinoma. Cancer Biol. Ther. *20*, 1127–1135.
27. Liu, X.X., Yang, Y.E., Liu, X., Zhang, M.Y., Li, R., Yin, Y.H., and Qu, Y.Q. (2019). A two-circular RNA signature as a noninvasive diagnostic biomarker for lung adenocarcinoma. J. Transl. Med. *17*, 50.
28. Li, S., Sun, X., Miao, S., Lu, T., Wang, Y., Liu, J., and Jiao, W. (2018). hsa_-circ_0000729, a potential prognostic biomarker in lung adenocarcinoma. Thorac. Cancer *9*, 924–930.
29. Zorn, A.M. (2001). Wnt signalling: antagonistic Dickkopfs. Curr. Biol. *11*, R592–R595.
30. Wang, W., He, Y., Rui, J., and Xu, M.Q. (2019). miR-410 acts as an oncogene in colorectal cancer cells by targeting dickkopf-related protein 1 via the Wnt/β-catenin signaling pathway. Oncol. Lett. *17*, 807–814.
31. Ma, Y.S., Lv, Z.W., Yu, F., Chang, Z.Y., Cong, X.L., Zhong, X.M., Lu, G.X., Zhu, J., and Fu, D. (2018). MicroRNA-302a/d inhibits the self-renewal capability and cell cycle entry of liver cancer stem cells by targeting the E2F7/AKT axis. J. Exp. Clin. Cancer Res. *37*, 252.
32. Feng, Y., Zhang, L., Wu, J., Khadka, B., Fang, Z., Gu, J., Tang, B., Xiao, R., Pan, G., and Liu, J. (2019). circRNA circ_0000190 inhibits the progression of multiple myeloma through modulating miR-767-5p/MAPK4 pathway. J. Exp. Clin. Cancer Res. *38*, 54.
33. He, R., Liu, P., Xie, X., Zhou, Y., Liao, Q., Xiong, W., Li, X., Li, G., Zeng, Z., and Tang, H. (2017). circGFRA1 and GFRA1 act as ceRNAs in triple negative breast cancer by regulating miR-34a. J. Exp. Clin. Cancer Res *36*, 145.
34. Wei, S., Zheng, Y., Jiang, Y., Li, X., Geng, J., Shen, Y., Li, Q., Wang, X., Zhao, C., Chen, Y., et al. (2019). The circRNA circPTPRA suppresses epithelial-mesenchymal transitioning and metastasis of NSCLC cells by sponging miR-96-5p. EBioMedicine *44*, 182–193.
35. Zhang, Z., Sun, L., Zhang, Y., Lu, G., Li, Y., and Wei, Z. (2018). Long non-coding RNA FEZF1-AS1 promotes breast cancer stemness and tumorigenesis via targeting miR-30a/Nanog axis. J. Cell. Physiol. *233*, 8630–8638.